Analysis of Reference Tidal Channel Plan Form For the Montezuma Wetlands Restoration Project

Sarah Pearce, Geomorphologist
Joshua N. Collins, Project Manager

San Francisco Estuary Institute
Contribution No. 80

May, 2004

ACKNOWLEDGEMENTS

We gratefully acknowledge Roger Leventhal of Far West Engineering, for his oversight and comments on this analysis and document. This project is a special study of the Montezuma Wetlands Restoration Project.

TABLE OF CONTENTS

INTRODUCTION AND PURPOSE

The Montezuma Wetlands Project will restore approximately 1,820 acres of tidal, seasonal, and managed wetlands in an eastern portion of Suisun Marsh where the Project site has been diked and used for agriculture for more than 100 years. The approximately 2,400 acre site is located on the eastern side of Montezuma Slough near the town of Collinsville, California in Solano County. As a result of perimeter levees that isolate the site from Bay-Delta tidal waters and the historical pumping of surface water off the site for agricultural purposes, the current surface elevations have subsided about 4-6 feet below sea level. Approximately 17 million cubic yards of sediment dredged from the San Francisco Bay-Delta will be used to raise surface elevations to conditions suitable for tidal marsh to be re-established at the site. Material dredged from the Bay-Delta (cover and noncover sediment suitable for restoration purposes) will be barged to the site, off-loaded, and placed in settling cells until target elevations are reached. The largest, primary tidal channels in each settling cell will be designed and constructed, with smaller channels allowed to develop naturally.

A need exists for accurate local data that quantifies tidal channel plan form measurements. A dataset specific to the North Bay, the larger Bay Area, or even a general dataset of this type has not been gathered or published. Successful wetland restoration will require data from surrounding wetlands to help inform and guide the design and construction of tidal marsh channels so that they mimic natural channels. Tidal channels with geometries similar to natural channels will function most like natural channels, allowing physical processes such as water and sediment transport, channel evolution and vegetation community development to occur. Accurately quantifying these metrics is one of many prerequisites for successful wetland restoration.

The purpose of this study is to collect information on channel plan form in tidal marsh areas adjacent to the Montezuma Wetlands Restoration Project site to help guide the design and construction of tidal marsh channels. Necessary metrics include channel plan form (channel width, and meander characteristics), drainage basin area, and confluence location and angle. The collected data will quantify the range of observed values for each metric analyzed, while also illustrating the natural variability of these tidal channel systems. The data will serve as a guideline to help design appropriate channels that have the functions of natural channels, including supporting the physical processes that occur in a dynamic tidal marsh system, and supplying diverse and adequate habitat for many species of plants and animals.

METHODS

Analysis of current and historic channel plan form focused upon map and aerial photograph interpretation, utilizing a series of aerial photographs and maps from many different sources and dates. Because these sources were already in electronic format, the methodology used on-screen interpretation rather than working off of physical hard copies. These electronic sources were analyzed in ArcView GIS, because this program enabled the easiest and most accurate measurement of channel features.

Sources

Although many other sources were gathered (including 1937 aerial photographs, 1866 USGS T-Sheet 1029, 1883 NOAA Suisun Bay Navigational map, and multiple years of 20th century NOAA Navigational maps) the primary data sources are the five listed in Table 1. In particular, the 1993 DOQQs (Digital Orthorectified Quarter Quadrangles) were the most utilized because the photographs are of a good resolution, and are registered and rectified, allowing direct and accurate measurement of channel features in ArcView. The 1989 NOAA Navigational map was utilized for confluence angle analysis and for determining channel order.

Table 1. Primary sources utilized for analysis.

Date	Agency	Data Type	Scale
1858	USCS	Napa Creek Plane Table Sheet T777	1:10,000
1980	USGS	7.5' Topographic quadrangles	1:24,000
1989	NOAA	Suisun Bay Navigational Map	1:40,000
1993	USGS	Digital Ortho Quarter Quadrangles	1:24:000
1995	NASA	Color infra-red aerial photographs	1:24,000

GIS Analysis

Channel plan form and angle of tributary confluences was measured using ArcView 3.2 software. The source data was added as a theme, then three new themes were created, "channel plan form metrics", "drainage basin areas", and "confluence angles". In each new theme, the relevant channel pattern was traced using the line tool. For registered and rectified sources, the line tool allows measurement of features because the length of each line segment, and the area of each polygon that is drawn are given by ArcView in meters (or square meters for polygon areas). As each metric was traced and measured, the line segment length or polygon area data was directly input into an excel spreadsheet.

Location and guidelines

Plan form analysis focused on wetland areas surrounding the Montezuma Wetlands Restoration Project site, wetlands near the mouth of the Napa River, and wetland areas on the northeast side of Suisun Slough (Figures 1, 2, and 3). Near Montezuma, measurements were made on Van Sickle, Wheeler, Simmons, Hammond and Grizzly Islands. Along the Napa River, measurements were made on Russ Island, Island No. 2, and in the area currently used as salt evaporators. Near Suisun Slough, measures were made in Rush Ranch, a historically undiked area. For the Suisun and Rush Ranch analyses, channels that were both shown on the 1989 NOAA map, and visible on the 1993 DOQQ photographs were analyzed. For the Napa analyses, channels larger than a single pen-line in width on the 1858 T-Sheet map were analyzed. Channel size ranges from single line channels on the maps that are generally first or second order channels, up to double line channels that are third or fourth order channels. Only systems that appeared to have a natural plan form were included. Locations of clear channel modification, straightening or diversion were not included. During analysis, each channel was numbered, to allow measurements to be revisited. Confluence locations were calculated only for confluences where a channel of a smaller order entered a channel of a larger order. Locations where two channels of the same order joined to form a larger order channel were not included.

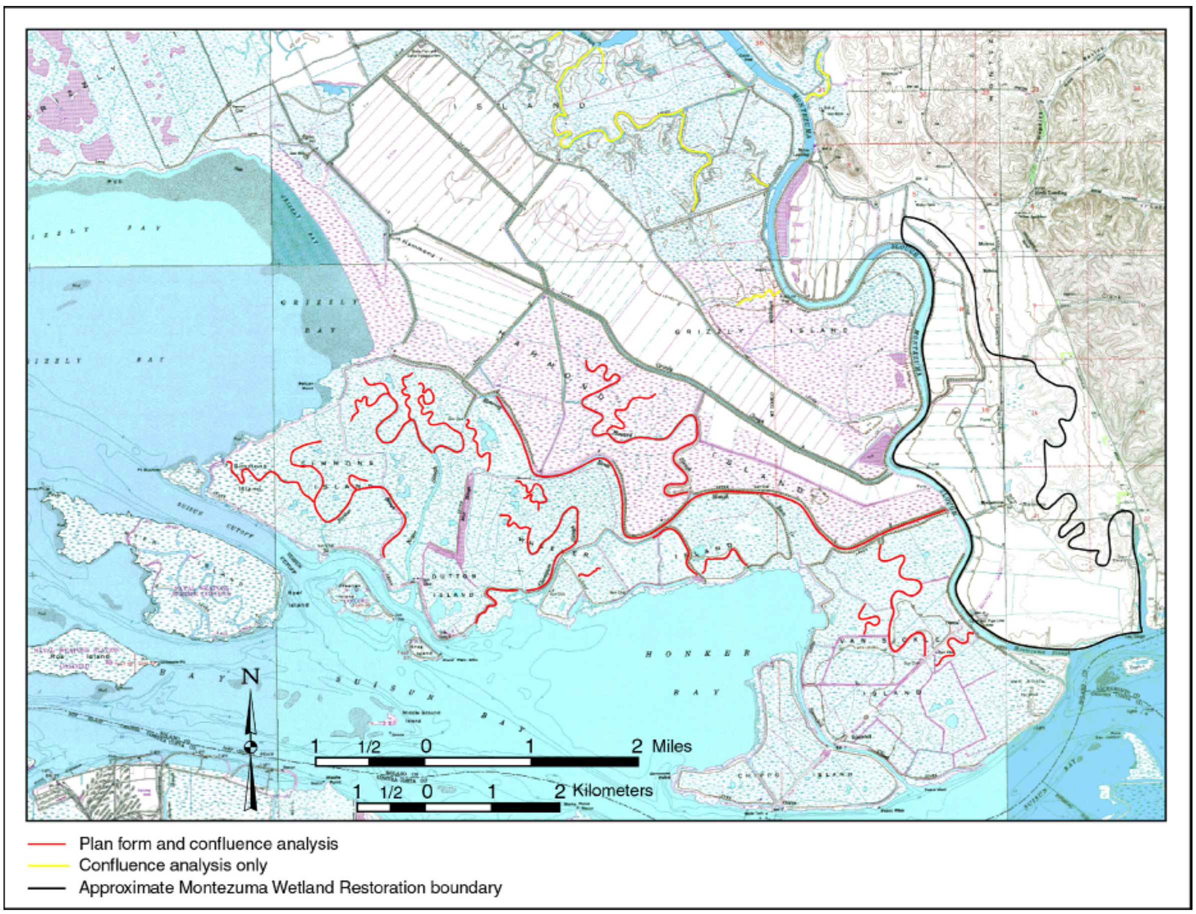

Figure 1. Location of Montezuma Wetland Restoration project and surrounding wetland systems. Approximate Montezuma Wetlands Restoration Project boundary shown in black. Tidal channels utilized for plan form analysis and confluence angle analysis are highlighted in red, while channels utilized only for confluence angle analysis are highlighted in yellow. Portions of the Honker Bay, Vine Hill, Denverton, and Fairfield South USGS 7.5’ topographic quadrangles shown.

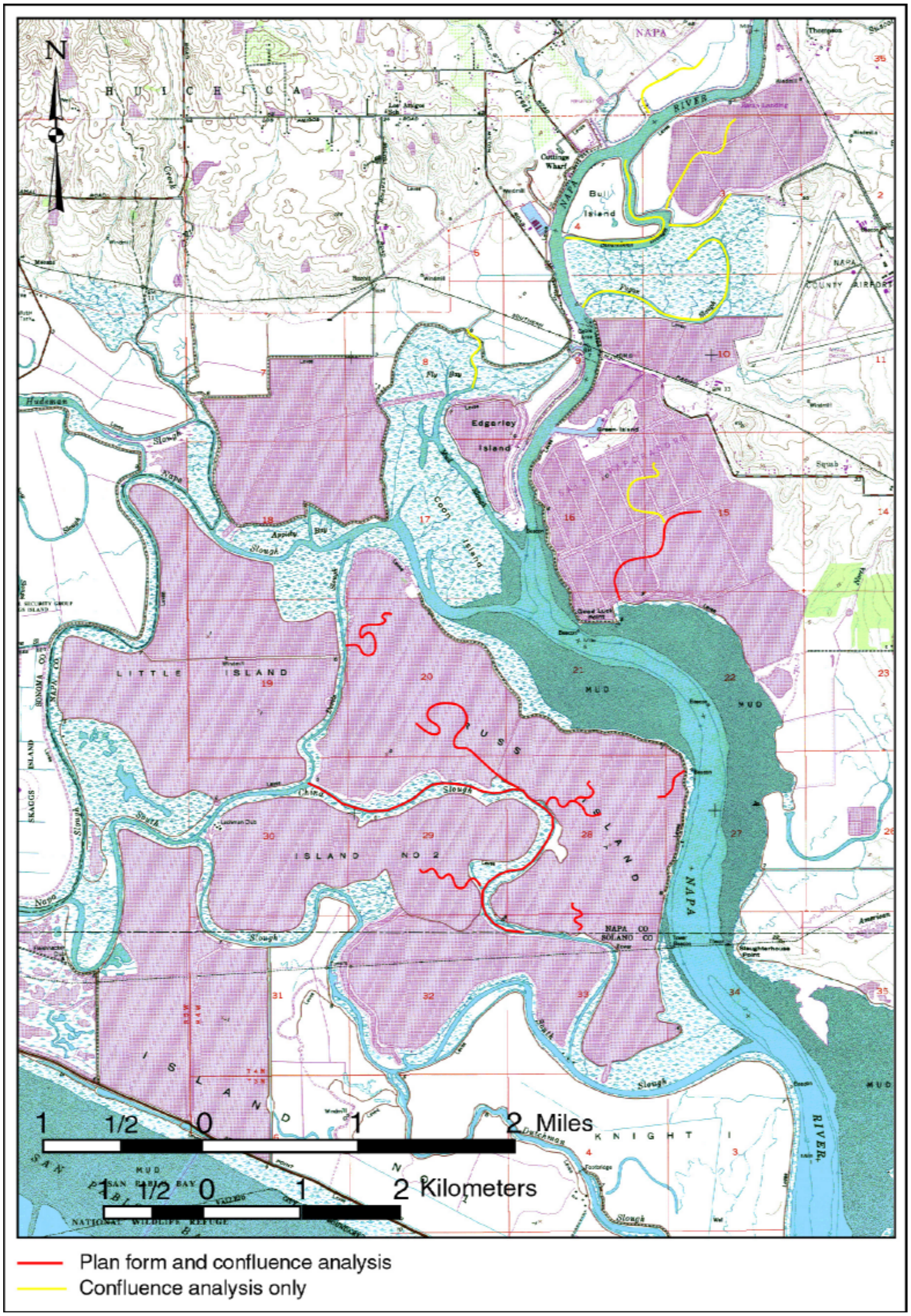

Figure 2. Location of wetland systems analyzed on the 1858 USGS T-Sheet map, near the Napa River. Tidal channels utilized in plan form analysis and confluence angle analysis are highlighted in red, while channels utilized only for confluence angle analysis are highlighted in yellow. A portion of the Cuttings Wharf USGS 7.5' topographic quadrangle is shown.

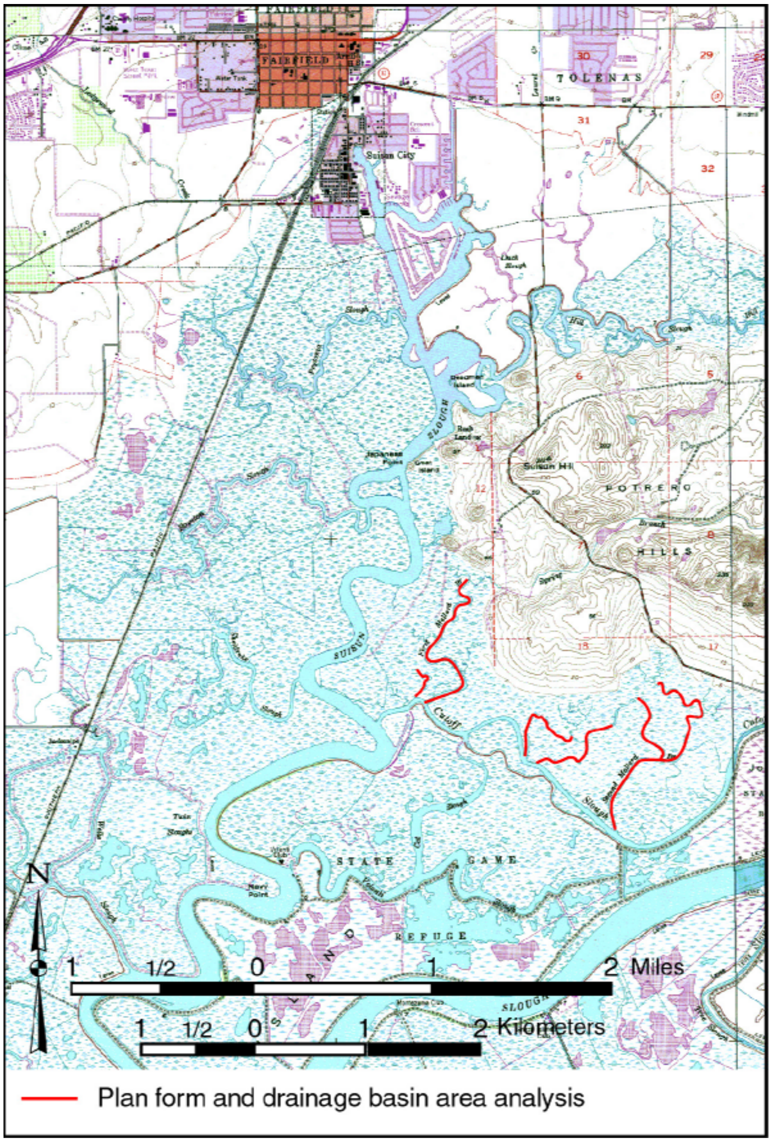

Figure 3. Location of wetland systems analyzed on the 1993 DOQQ aerial photographs in the Rush Ranch area, near the town of Fairfield and the Suisun Slough. A portion of the Fairfield South USGS 7.5' topographic quadrangle is shown.

Measured Channel Plan Features

Utilizing the gathered data sources, primarily the 1993 USGS DOQQs, the following channel metrics were measured and quantified: Average channel width (one measure taken upstream and downstream of the meander, then averaged), radius of curvature for each meander (measured using the chord and middle ordinate method), meander wavelength, meander amplitude, and meander belt width (Figure 4). An example from the Suisun area shows the traced meanders and associated measured geometries overlying the DOQQ (Figure 5).

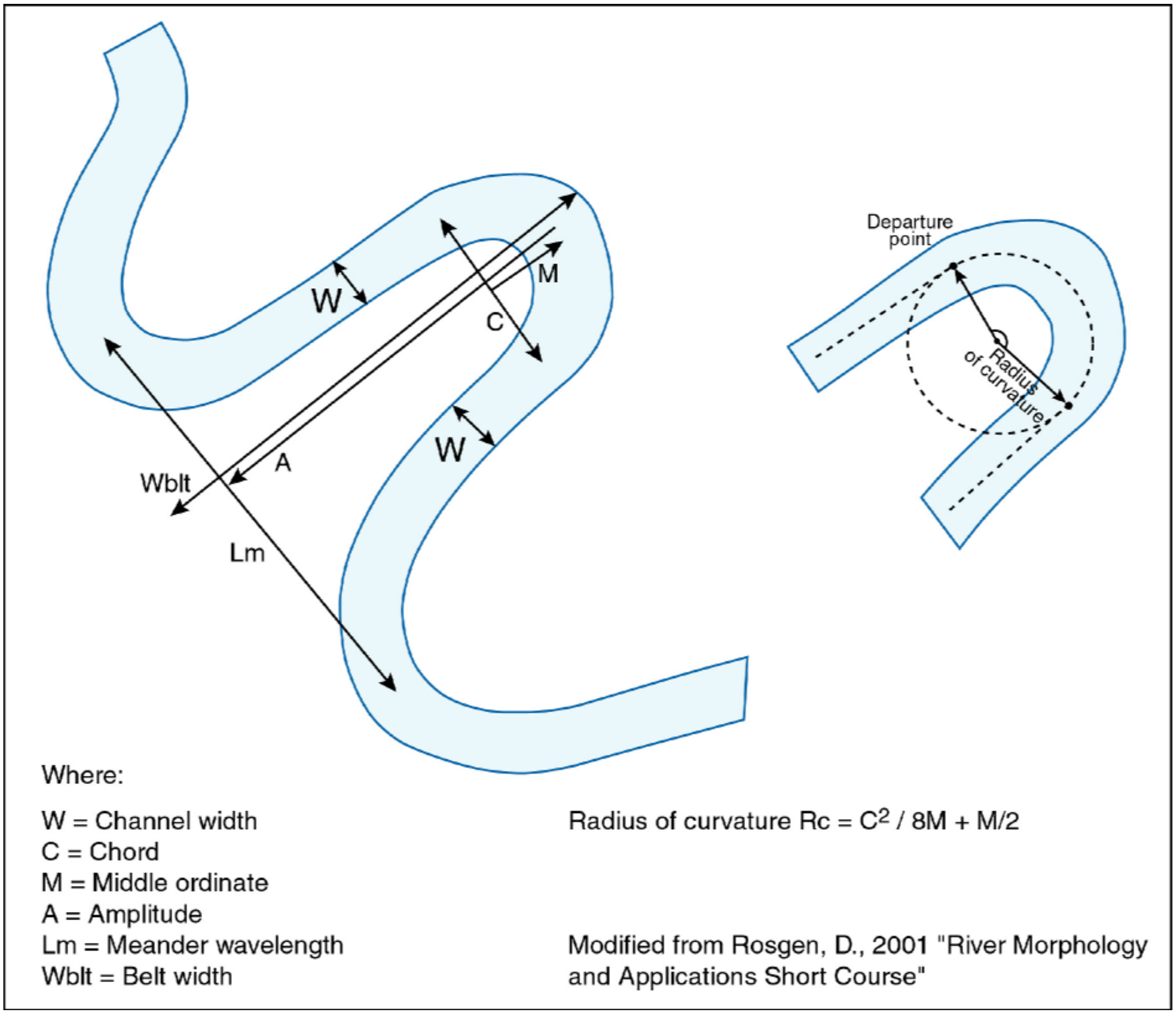

Figure 4. Measured channel plan features.

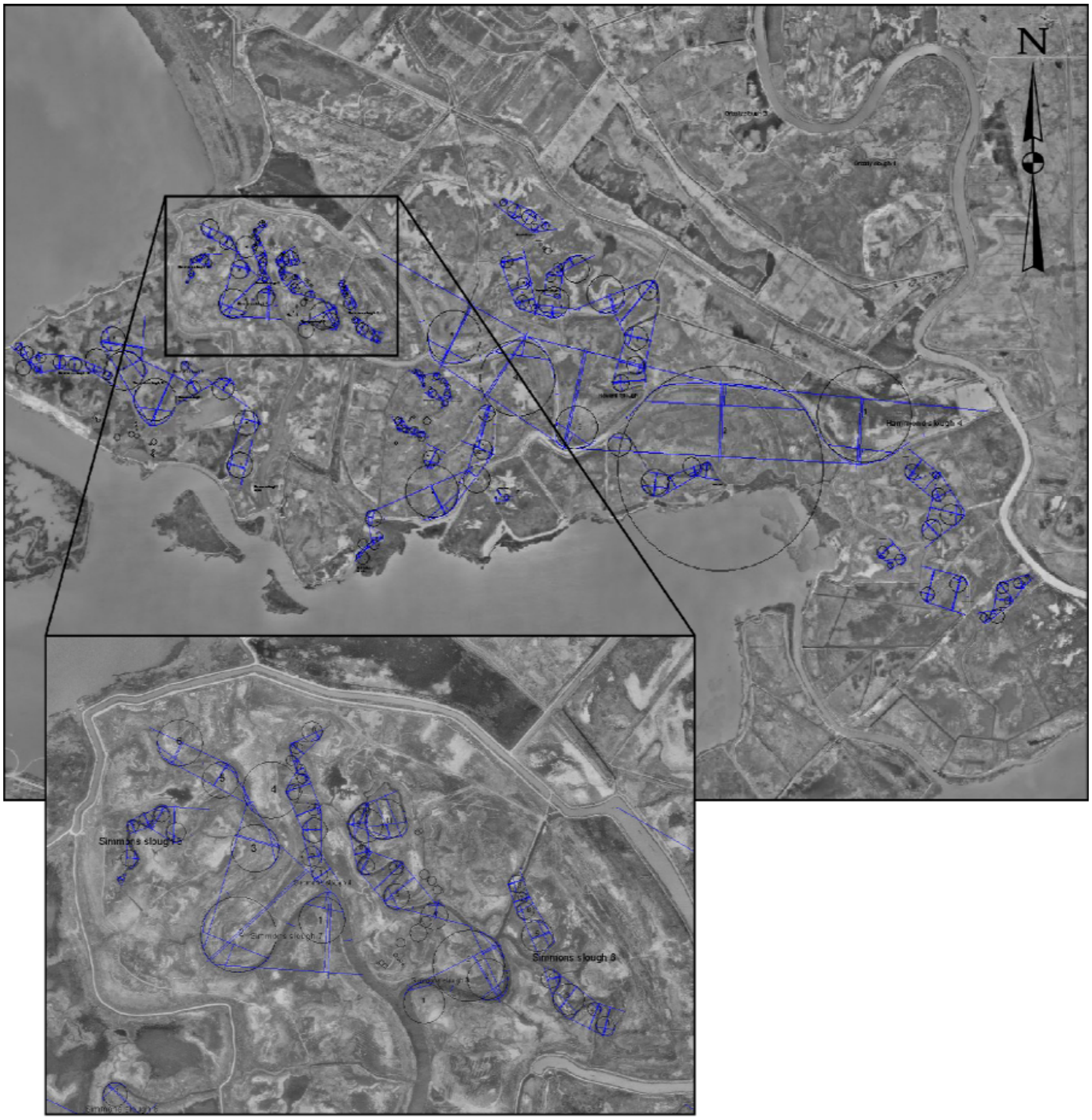

Figure 5. Portion of the 1993 USGS DOQQ with traced meanders and measured plan form geometries overlying the image. Inset is a close-up of measures made on Simmons Island.

Measured Confluence Features

Besides channel plan form analysis, this study also focused upon quantifying the location of tributary channel confluences. Casual observation noted that wetland tributary channels often join a larger channel at the outside of a meander of that channel. This analysis evaluates and quantifies confluence locations in wetland areas also analyzed for plan form metrics.

Defining where along a curve a tributary enters is not a standard geomorphic metric. However, Leopold (1994) published an equation that describes the angle of deviation of a meandering channel compared to the downstream direction. The plot of the angle of deviation as a function of distance along the channel yields a sine-generated curve. Using this concept as a model, we created a methodology to quantify the confluence location. Figure 6 is a simplified sketch to illustrate how measures were made. First, the generalized downstream direction of the larger mainstem channel was visually estimated and defined. Then, at the location of a tributary confluence, a shorter line was drawn to represent the direction of flow of the mainstem at that discrete point. This shorter line was compared to the line representing the generalized downstream direction, and the angle between the two was measured.

For example, in Figure 6, the first panel illustrates a tributary entering exactly on the outside of a meander. At this point, flow in the mainstem is flowing in exactly the same direction as the generalized downstream direction. The two lines are parallel, giving an angle of 0°. The last panel illustrates the other extreme; in this case, the tributary enters along the straight portion, between two meander bends. Here, flow in the mainstem is exactly perpendicular to the general downstream direction, giving an angle of 90°. The middle panels show examples from cases in between the two extremes, illustrating 30° and 60°. Any angle between 0° and 90° is possible. This analysis also differentiated between the upstream and downstream sides of a meander. Downstream is defined as the direction towards greater tidal influence. For any given meander, a tributary was defined as upstream if it entered on the upstream side of the curve (ranging from 90° to 0°). The downstream side of the curve captures those locations ranging from 0° back up to 90°. Only upstream examples are shown in Figure 6.

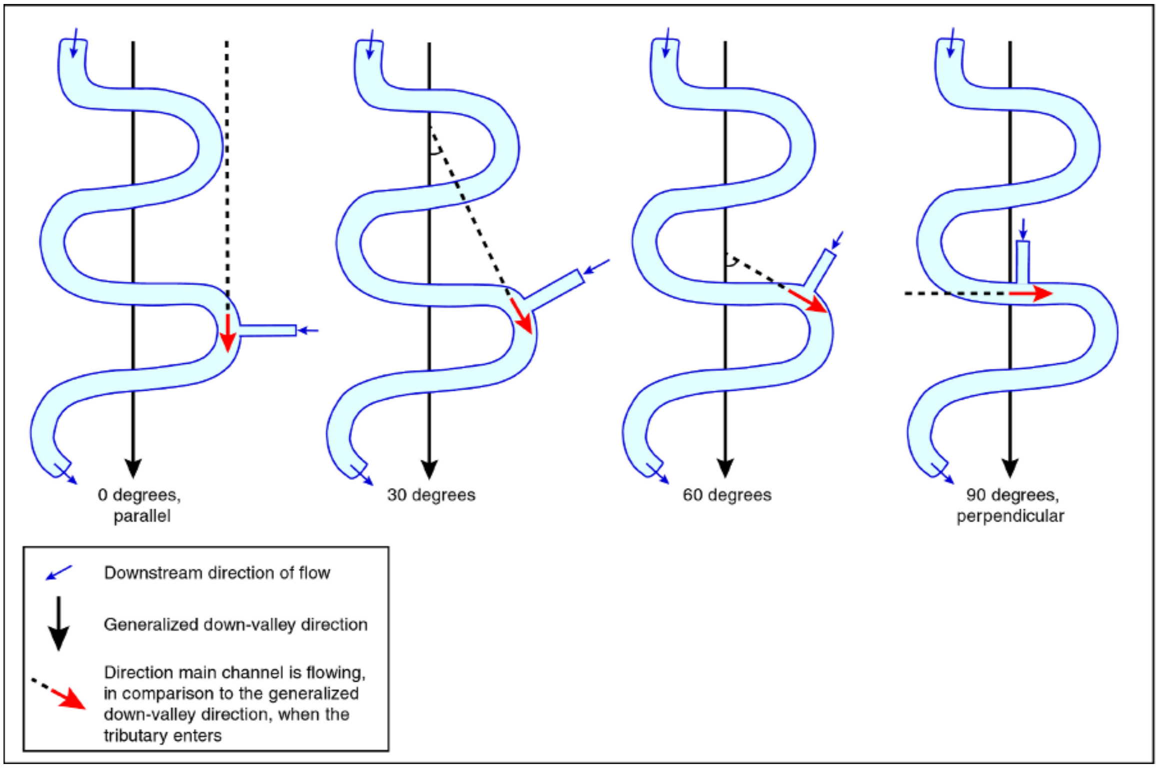

Figure 6. Simplified sketch illustrating the variable location of tributary confluences along the larger mainstem channel meander. Measurement of confluence location (in degrees) compares direction of flow in the mainstem at that discrete location to the generalized downstream flow direction.

Data was collected using the 1993 USGS DOQQs, the 1989 NOAA Navigational map, and the USCS Napa T-Sheet. In ArcView in the "confluence angles" theme, a line was drawn to represent the general downstream direction of the larger, mainstem channel. Then a smaller line was traced to show the direction the mainstem is flowing at the discrete location where a tributary enters. Then an ArcView routine was used to calculate the angle between the two lines (CalculateAngleofIntersection.avx). This data was then directly input into an excel spreadsheet.

Issues of scale

This analysis utilized maps and photographs of many different scales. Larger-scale sources show a greater level of detail, including many of the smallest tidal channels, in comparison to smaller-scale sources (Figure 7). The issue of scale was important to address before beginning any analysis.

In the Napa area, channels were ordered using the USCS T-Sheet. In the example shown in Figure 7, the smallest channels are first order channels. However, because only second order and larger channels are shown with a double pen-line, channel plan form metrics were only measured for second order and larger channels. In the Suisun area, channels were ordered using the 1989 NOAA map. However, after collecting a substantial amount of data, a decision was made to modify the ordering of these channels. Firstly, this map has a low level of detail, and clearly does not show many of the smaller tidal channels. Secondly, after comparing the measured width of channels to field experience, and to widths measured in the Napa area, a disparity between the width and channel order was noticed. To rectify this problem, channel order for each channel was increased by one. For example, in Figure 7, although the small channels on the left side of the NOAA map theoretically should be first order channels, we increased the order to second order. This adjustment brought the width dataset inline with what is typically observed in wetland systems around the Bay Area.

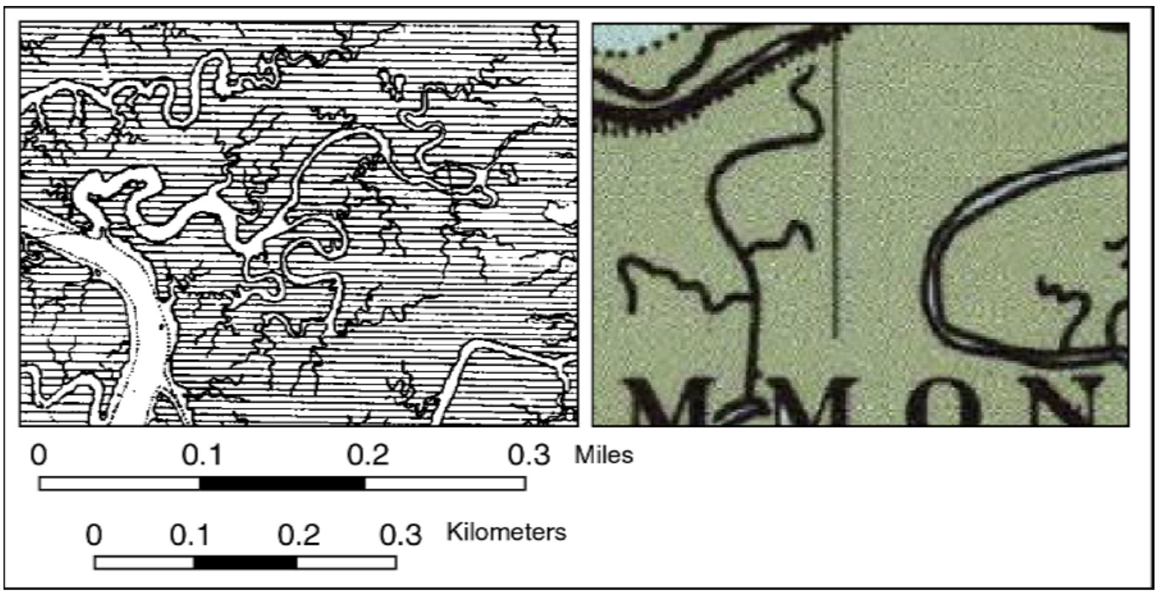

Figure 7. Example showing the two scales at which tidal channels have been mapped. On the left is an area from the 1858 USCS Napa T-sheet, and on the right is an area from the 1989 NOAA Navigational map, shown at the same scale. Notice the level of detail to which channels are mapped.

RESULTS

Analysis of each channel metric reveals that natural tidal channels in the Suisun, Rush Ranch, and Napa areas have a wide range of values. However, for each metric, a trend is typically evident. The following graphs define the range of values observed in these wetland systems.

Channel width

Channel width is a basic unit of measure for a channel. Channel width and depth are uniquely adjusted to the volume of water transported by the channel reach. Width is related to channel order and many plan form metrics. For example, Figure 8 shows the relationship between channel width and channel order. Not surprisingly, channels of a higher order are generally wider. Although a fair amount of variability exists, the average value for channel order does increase for each order.

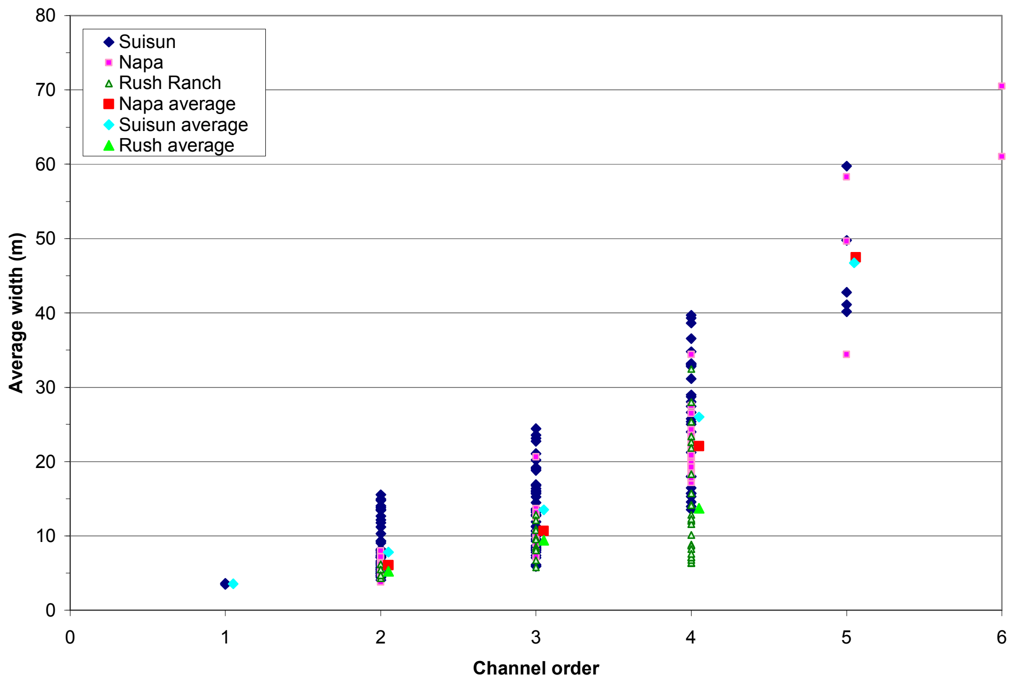

Figure 8. Graph showing channel order versus average channel width (in meters). Average values for each channel order for the Suisun, Rush Ranch, and the Napa data are also shown.

Radius of curvature

Radius of curvature (Rc) is a basic measure that relates to the size and shape of channel meanders. It is defined as the radius of the circle of curvature, or osculatory circle, at any point of a curve (www.dictionary.com, April, 2004). In this analysis, it was calculated using the chord and middle ordinate method (see Figure 4). Radius of curvature relates to channel width (and thus, channel order) (Figures 9 and 10), as well as to meander wavelength (Figure 11). As the meander wavelength increases, so must the radius of curvature.

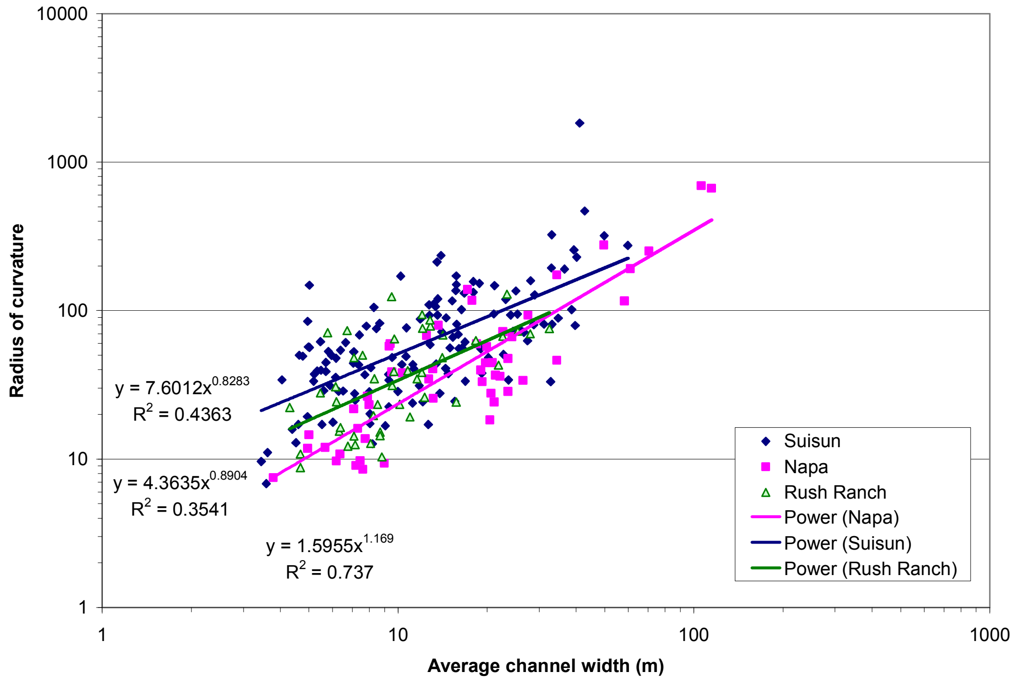

Figure 9. Graph of average channel width versus radius of curvature (Rc). Power trend lines and equations are shown.

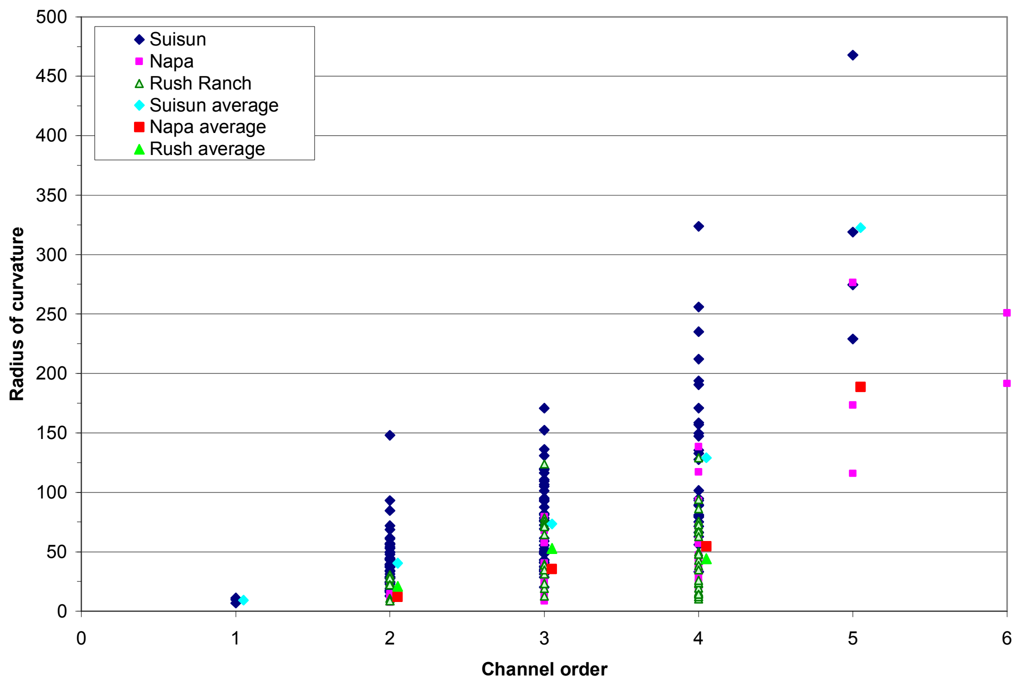

Figure 10. Graph of channel order versus radius of curvature (Rc). Average values for each channel order are also shown.

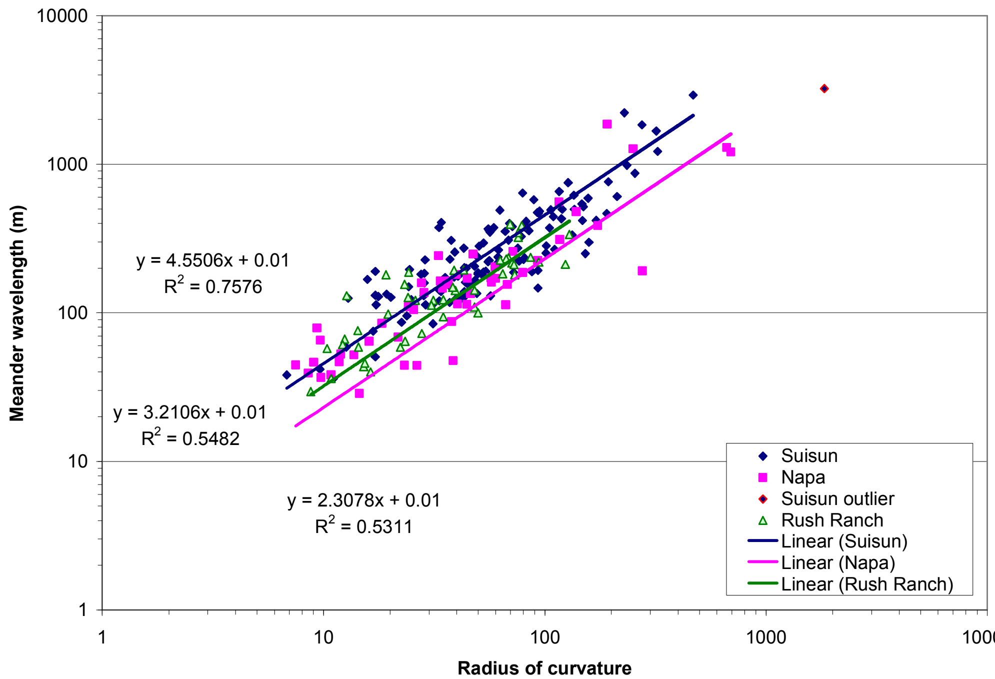

Figure 11. Graph of radius of curvature (Rc) versus meander wavelength. Linear trend lines and equations are shown. The single Suisun outlier data point is not included in the trend line.

Wavelength and amplitude relationships

Wavelength and amplitude are the basic measures defining the meander pattern of a channel. These metrics are generally related to channel width and order, with larger channels having larger meander patterns. The channel width and meander wavelength relationship is shown in Figure 12, while the width and amplitude relationship is shown in Figure 13. Both wavelength and amplitude are linearly related to width, however amplitude has a considerable amount of scatter about the best-fit line. Figure 14 illustrates the large amount of scatter in the dataset when plotting meander wavelength versus amplitude. In general, the Napa data tend to form more of a linear relationship, whereas the Suisun and Rush Ranch data form a cloud of data points with no clear trend.

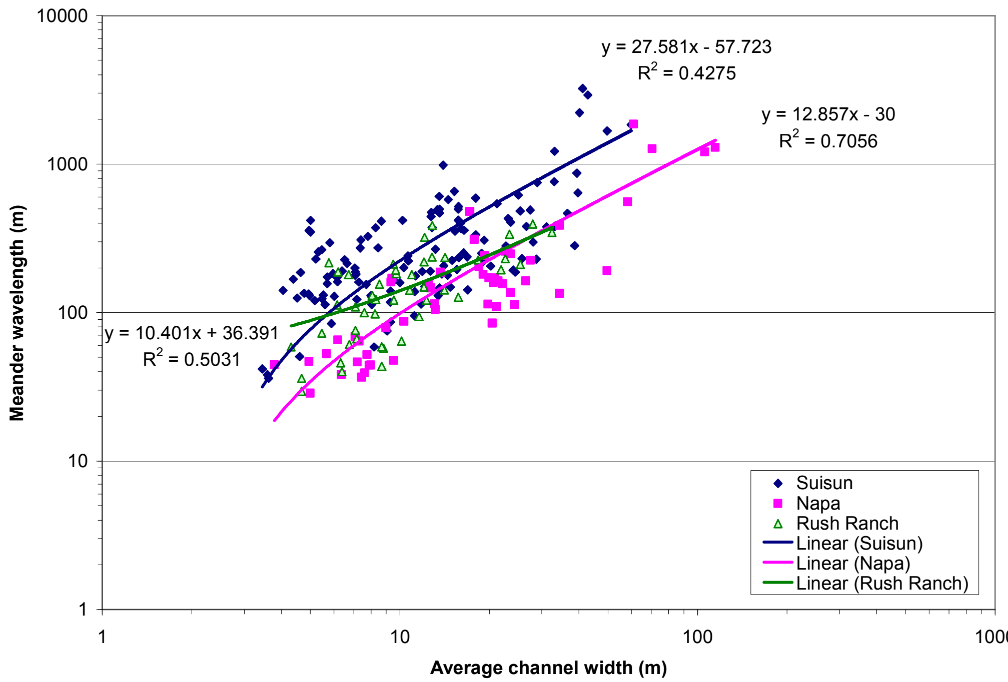

Figure 12. Graph of average channel width versus meander wavelength. Linear trend lines and equations are shown.

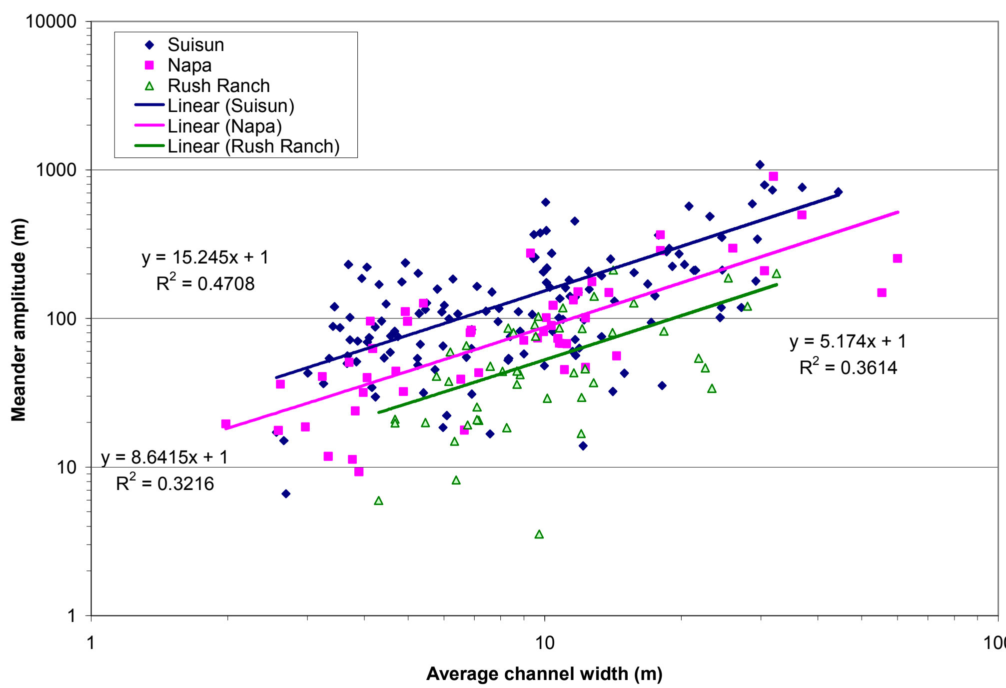

Figure 13. Graph of average channel width versus meander amplitude. Linear trend lines and equations are shown.

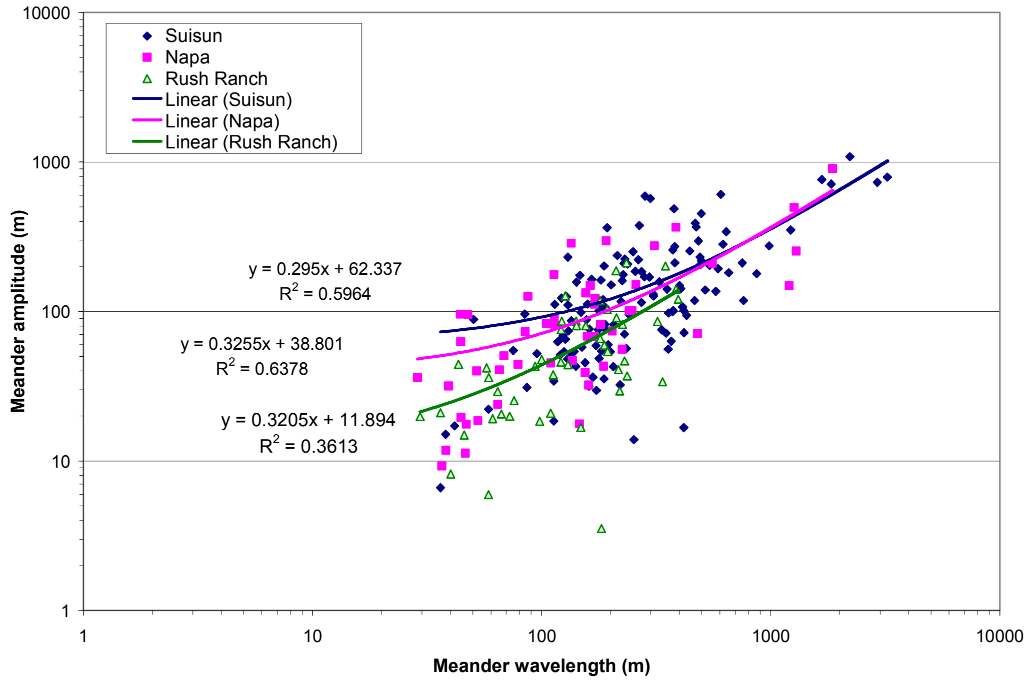

Figure 14. Graph of meander wavelength versus meander amplitude.

Tributary confluence angle measures

The location of where a tributary joins the mainstem along a meander curve can be quite variable. However, this analysis shows that for the observed tidal channel systems, tributaries do typically join on the outside of a meander bend, at a location where the mainstem flow only deviates from the downstream direction most often between 0 and 30°. The same data set is plotted in Figures 15 – 17, utilizing different "bin" categories; Figure 15 is plotted using 5° bins, Figure 16 is plotted using 10° bins, and Figure 17 uses 30° bins. Figure 18 also uses the same data set, however, channel order and orientation along the curve (upstream or downstream) are shown. Data is plotted for each channel order, with tributary confluences that occur on the upstream side of a meander bend plotted as positive numbers, and confluences that occur on the downstream side of a meander plotted as negative numbers.

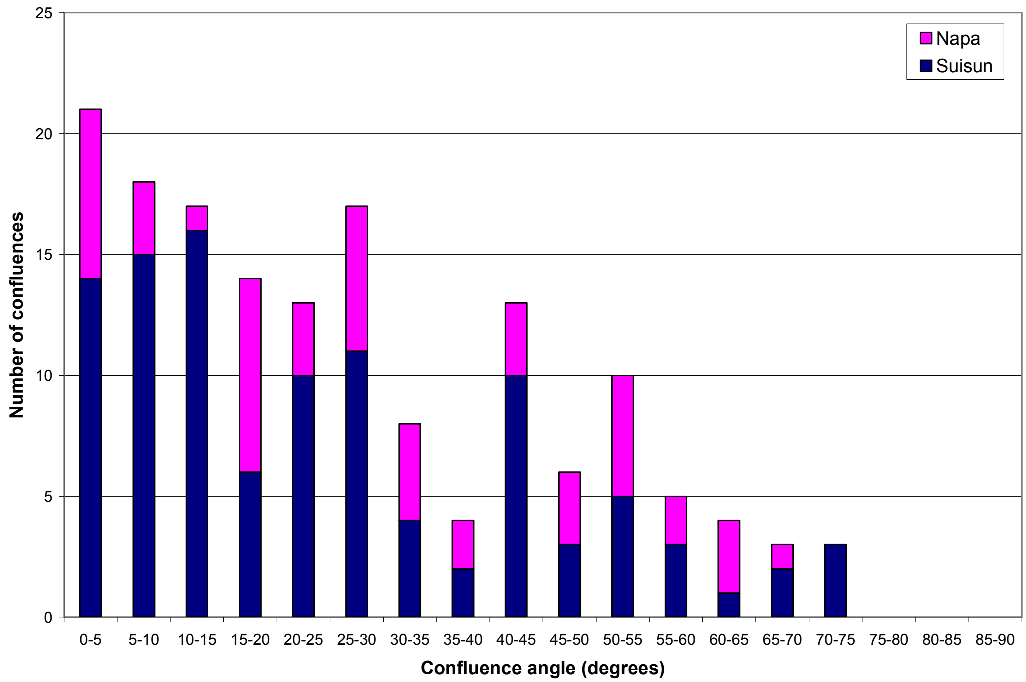

Figure 15. Plot of tributary confluence angle (in 5 degree bins) versus number of confluences.

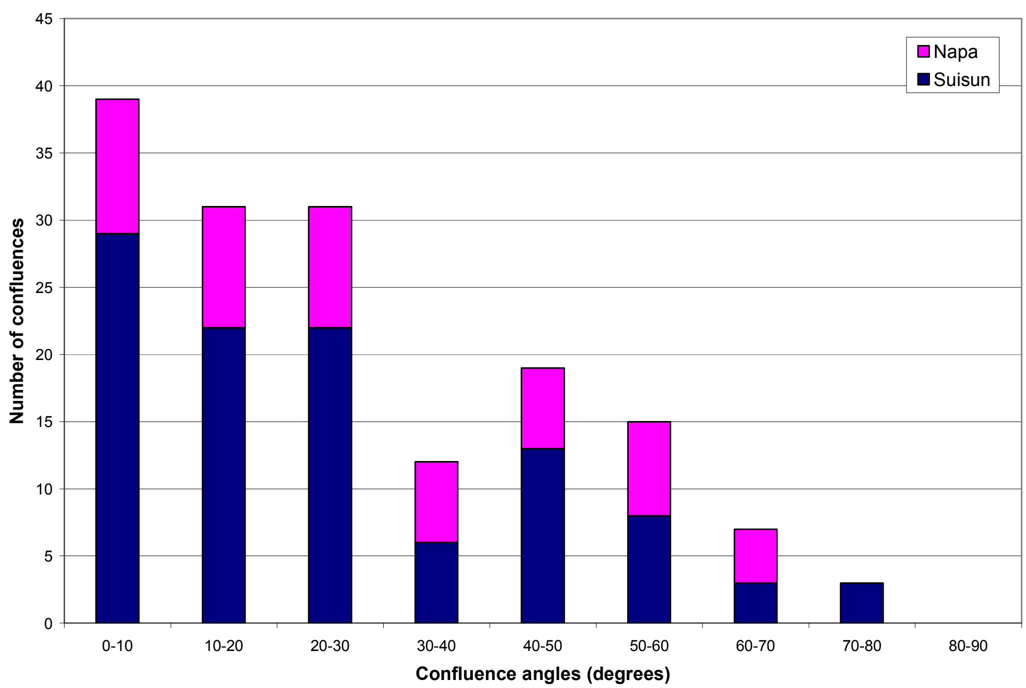

Figure 16. Plot of tributary confluence angle (in 10 degree bins) versus number of confluences.

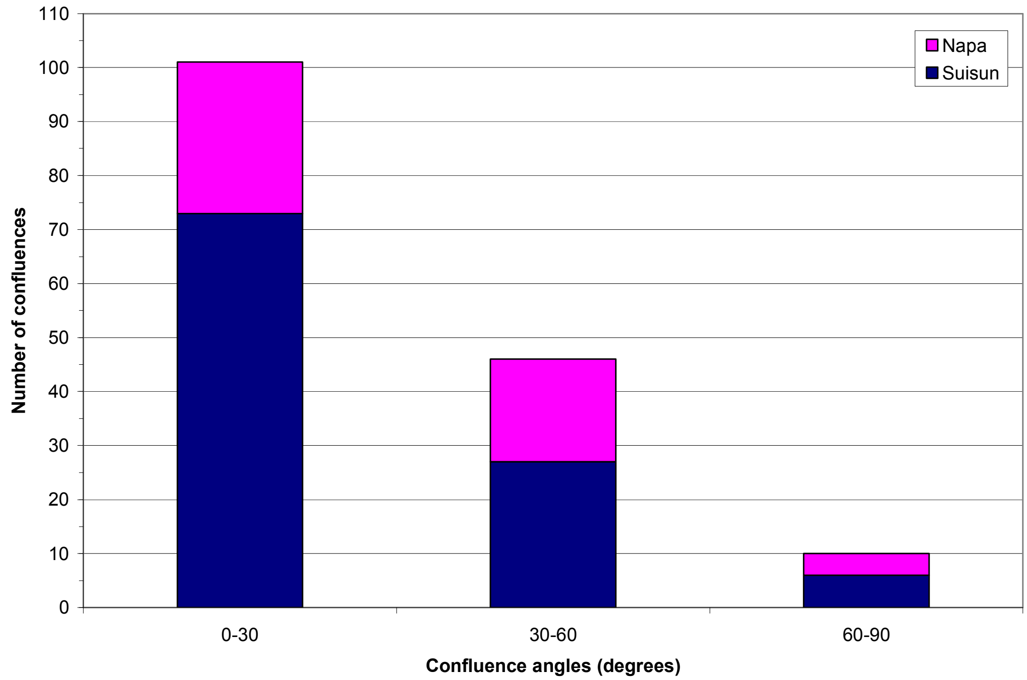

Figure 17. Plot of tributary confluence angle (in 30 degree bins) versus number of confluences.

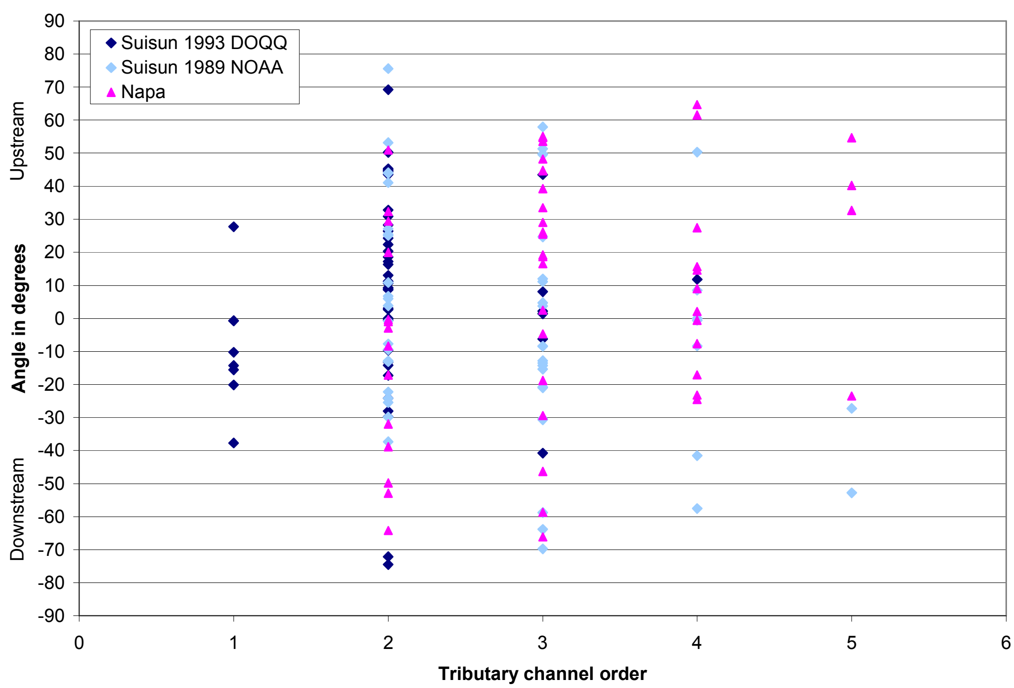

Figure 18. Graph of tributary channel order versus confluence angle. Positive values represent confluences on the upstream side of a meander, whereas negative values represent confluences on the downstream side of a meander (see Figure 6).

Drainage basin area

As channel order increases, the area drained by those channels will also increase. Figure 19 shows the increasing drainage basin area (in acres) with increasing channel order. Data from Napa, Suisun, and Rush Ranch are shown. Similarly to the other metrics analyzed, the Napa and Rush Ranch datasets are plotting slightly lower than the Suisun dataset.

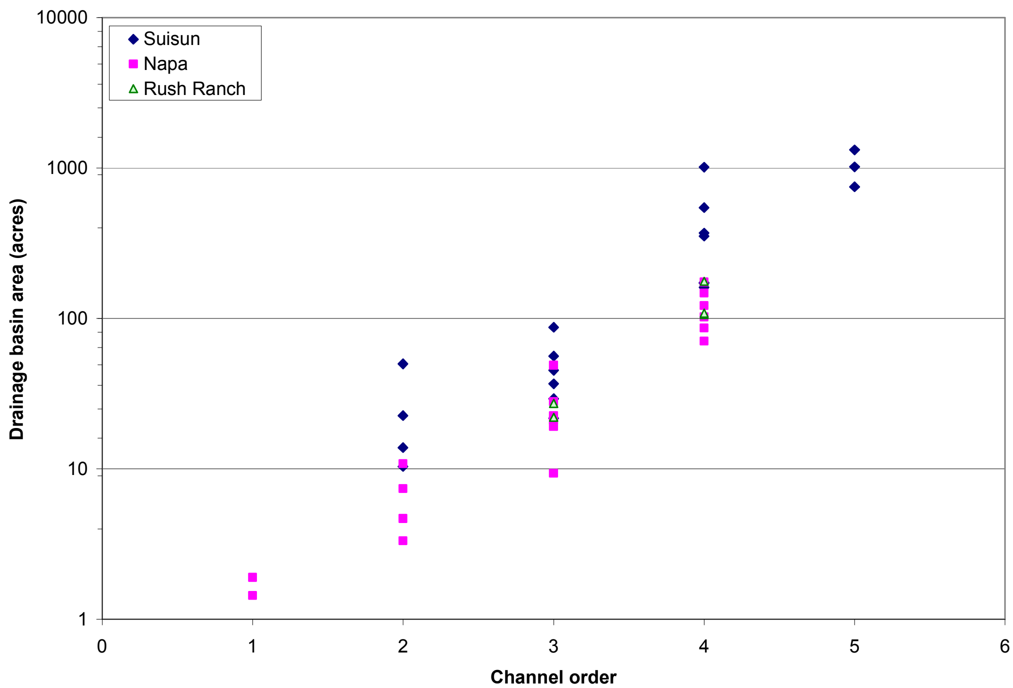

Figure 19. Graph showing channel order versus drainage basin areas, in acres.

CONCLUSIONS

Wetland areas adjacent to the Montezuma Wetlands Restoration Project site near Suisun Bay, Rush Ranch, and near the Napa River, represent analogue models for natural channel plan form patterns. Analyzing these neighboring systems and collecting data on plan form and tributary confluence metrics provides a local data set to help guide the design of new channels. Modeling new constructed channels on existing natural channels increases the likelihood of success; that is, encouraging the functioning and physical processes found in natural channels.

Relationships between channel width and order, the radius of curvature, and meander wavelength and amplitude are observed and quantified. Generally, average channel width increases with order. Most of the metrics are linearly related, with the datasets from the

Napa and Rush Ranch areas typically plotting slightly lower than the dataset from the Suisun area. The data illustrate the range of natural channels in each of these measured metrics. Additionally, it appears that most tributary confluences occur on the outside of meander bends, with most occurring between 0 and 30° deviation from the generalized downstream direction of mainstem flow.

REFERENCES

Leopold, L., 1994. A View of the River. Harvard University Press, Cambridge, Massachusetts. 298 pp.

NASA, 1995. Color infra-red aerial photographs-SFB. Acquired for the San Francisco Bay Watershed Database. NASA, Seattle, Washington. 1:24,000.

NOAA, 1989. Suisun Bay Navigational Map, chart 5534. U.S. Department of Commerce, Washington, D.C. 1:40,000.

Rosgen, D., 2001. River Morphology and Applications Short Course Handbook. Pagosa Springs, CO.

United States Coast Survey (USCS), 1858. Napa Creek and Napa City California, Plane Table Sheet XXXII, Register No. T777. 1:10,000.

USGS, 1993. Digital Ortho Quarter Quadrangles, 1:24,000.

USGS, 1978. Antioch North, CA 7.5' Topographic quadrangle, 1:24,000. United States Geological Survey, Denver, Colorado.

USGS, 1949. Cuttings Wharf, CA 7.5' Topographic quadrangle, 1:24,000. United States Geological Survey, Denver, Colorado.

USGS, 1953. Denverton, CA 7.5' Topographic quadrangle, 1:24,000. United States Geological Survey, Denver, Colorado.

USGS, 1949. Fairfield South, CA 7.5' Topographic quadrangle, 1:24,000. United States Geological Survey, Denver, Colorado.

USGS, 1953. Honker Bay, CA 7.5' Topographic quadrangle, 1:24,000. United States Geological Survey, Denver, Colorado.

USGS, 1959. Vine Hill, CA 7.5' Topographic quadrangle, 1:24,000. United States Geological Survey, Denver, Colorado.